

Hysteretic whirl stabilization in rotor-shaft-bearing systems on dry friction suspension

Francesco Sorge, Marco Cammalleri

Department of Mechanics, University of Palermo, Italy
E-mail: sorge@dima.unipa.it, cammalleri@dima.unipa.it

Keywords: Dry friction suspension, hysteretic instability, rotating machinery.

SUMMARY. The undesired whirl of rotating machines can be reduced by elastic journal box suspension systems equipped with dry friction dampers. The critical speeds can be cut off by the adhesion of the friction surfaces and the whirl amplitude can be restrained throughout the remaining sliding range by a proper choice of the suspension-to-shaft stiffness ratio and of the support-to-rotor mass ratio. The dry friction forces counteract also efficiently the well known destabilising effect of the shaft hysteresis in the supercritical range. This lecture deals firstly with the natural precession speeds, investigates the steady response to unbalance and defines the ranges of adhesive or sliding contact. Then, the stabilisation “in the small” of the hysteretic whirl by means of other external dissipative sources is studied applying the Floquet approach through a perturbation procedure, while the stability “in the large” is checked by the direct numerical solution of the motion equation.

1 INTRODUCTION

Dangerous whirling motions may arise in a rotor-support system when approaching the critical flexural speeds, and a great deal of previous studies have focused on this technical problem and on the strategy to face it. Flexible-damped supports have been widely analyzed (see [1-4]), but such additional sources of dissipation remain active and absorb power also at the operating point.

Previous analyses of the authors have developed the idea of suspending the journal boxes on elastic supports with suitable rubbing surfaces orthogonal to the shaft axis, in order to damp the critical whirling by dry friction, both for symmetric or asymmetric constraint configurations [5-6]. The wear compensation of the sliding surfaces can be made in practice automatic if the friction pads are loaded by suitable spring devices (e. g. Belleville washers, that may keep a nearly constant closure force when properly designed: see also patents [7-8]).

This suspension configuration operates quite efficiently if the adhesive state is planned to include the usual working condition of the rotating machine, whilst the sliding operation starts spontaneously to quench the whirl when approaching the critical speeds of the fixed-support system. The dry friction dampers behave thus similarly to clutches, which either lock or release the connection between the journal boxes and the frame depending on the rotational speed, and do not produce significant increase of power dissipation or heat production because the friction devices are mostly motionless.

On the other hand, a relevant drawback of rotating machinery is the typical trend to instability in the supercritical range due to the shaft material hysteresis, which may be restrained however by other external dissipative sources [9-10]. The hysteresis effect may be dealt with by introducing an equivalent coefficient of viscous damping, inversely proportional to the whirling frequency, and assuming that the hysteretic force is given by the product of this coefficient and the rotor centre velocity relative to a reference frame rotating rigidly with the shaft end section.

In particular, the stabilising effect “in the small” of the external dissipation may be studied by some perturbation approach. As the rotating system behaviour is non-linear due to dry friction, the perturbed motion equations contain periodic time-dependent coefficients, whence the Floquet approach must be used and the stability must be checked by controlling the magnitude of the Floquet characteristic multiplier. However, for large dry friction levels on the supports, the Coulombian forces exert a very strong stabilising effect “in the large”, as can be ascertained by the numerical solution of the full motion equations, and the final non-periodic trajectories run very close to the steady unstable trajectories.

2. MATHEMATICAL MODEL

The mathematical model is similar to reference [6]. The differential system is non-linear because of the continuous self-aligning of the sliding friction forces in opposition to the variable directions of the instantaneous sliding velocities and moreover, the sliding conditions may happen to be replaced by adhesive conditions, in correspondence of one or both supports, in some portions of the speed range. Nevertheless, for axisymmetric stiffness and damping of the shaft and the supports, a steady circularly polarized solution may be obtained straightforwardly in closed form.

A scheme of the rotor-suspension system is shown in Figure 1 and may be used as a reference

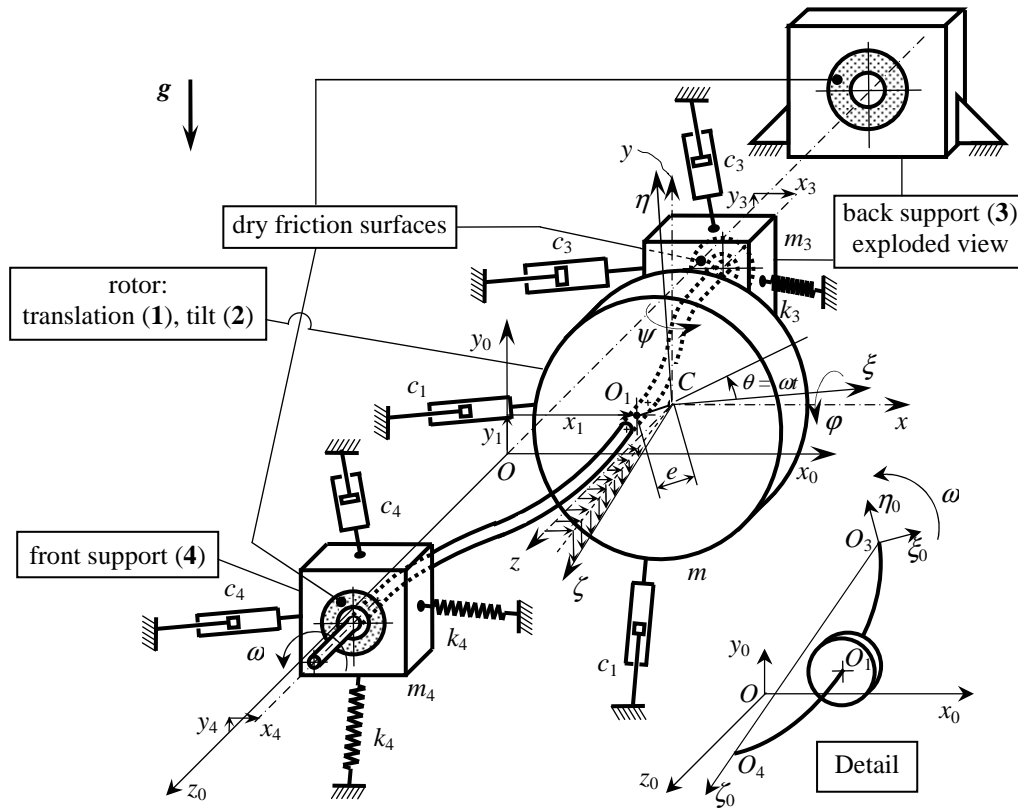


Figure 1: Scheme of rotating machine with exploded view of back support and frame.
Detail: reference system rotating with end sections

for the notation. The rotor mass centre C is eccentric at a distance e from the intersection O_1 of the shaft line with the rotor central cross-section. The moving frame $C\xi\eta\zeta$ does not take part in the main rotating motion with angular speed ω , but only performs the small elastic rotations φ and ψ around the axes x and y . The shaft is horizontal and the gravitational field \mathbf{g} is counter-directed with respect to the y axis.

Some external viscous-like environmental dissipation is assumed to affect the translational and rotational motions of the rotor and the translational motion of the supports, whence the damping coefficients c_1, c_3, c_4 [N×s/m] (translative) and c_2 [N×s×m] (rotative) are introduced.

On the other hand, the shaft hysteresis produces an internal dissipative force on the rotor in opposition with the velocity $\mathbf{v}_{\text{rel.}}$ of point O_1 relative to a reference frame $O_3\xi_0\eta_0\zeta_0$ containing the centres of the shaft end sections and rotating with the shaft angular speed ω (detail of Fig. 1). Indicating the dimensionless distances of the rotor from the shaft ends with $L_3 = -z_3/l$ and $L_4 = z_4/l$, where l is the shaft length, the components of $\mathbf{v}_{\text{rel.}}$ in the fixed reference $Ox_0y_0z_0$ are $v_{\text{rel.,}x} = \dot{x}_1 - \dot{x}_3L_4 - \dot{x}_4L_3 + \omega(y_1 - y_3L_4 - y_4L_3)$ and $v_{\text{rel.,}y} = \dot{y}_1 - \dot{y}_3L_4 - \dot{y}_4L_3 - \omega(x_1 - x_3L_4 - x_4L_3)$. The hysteretic force on the rotor is expressed by the product of this velocity and a hysteretic coefficient c_h : $\mathbf{F}_h = -c_h\mathbf{v}_{\text{rel.}}$, while the forces on the supports are $\mathbf{F}_{3h} = -L_4\mathbf{F}_h$, $\mathbf{F}_{4h} = -L_3\mathbf{F}_h$.

Defining a reference stiffness of the shaft with k (e. g., one may put $k = 48EI/l^3$ for self-aligning bearings), and a reference critical speed with $\omega_c = \sqrt{k/m}$, the dimensionless ratios $\Omega = \omega/\omega_c$, $M_3 = m_3/m$, $M_4 = m_4/m$, $K_3 = k_3/k$, $K_4 = k_4/k$, and the damping factors $d_{1,3,4} = 0.5c_{1,3,4}\omega_c/k$ and $d_2 = 0.5c_2\omega_c/(kl^2)$ are introduced, together with the dimensionless gravity parameter $\Gamma = mg/ek$.

In the case of a weighty, perfectly balanced rotor, the motionless equilibrium deflection plane counter-rotates with the angular speed $-\omega$ with respect to the rotating frame $O_3\xi_0\eta_0\zeta_0$ of Figure 1. Therefore, assuming the hysteretic work proportional to the cycle area, i. e. assuming the integral $c_h \oint (v_{\text{rel.,}x}^2 + v_{\text{rel.,}y}^2) dt = c_h \omega \oint [(y_1 - L_4y_3 - L_3y_4)_{\text{equil.}}^2 + (x_1 - L_4x_3 - L_3x_4)_{\text{equil.}}^2] d\theta$ proportional to the square of the path radius of point O_1 independently of ω , one deduces that the product $h = c_h\omega$ may be considered constant on varying ω (h : hysteresis constant of the material) and a constant hysteresis factor $d_h = 0.5h/k$ can be introduced. In the presence of some unbalance, either static or dynamic, a further steady shaft deflection has to be superimposed, on a plane which rotates rigidly with the shaft angular speed ω , and is thus uninfluential on the overall hysteretic dissipation. When analysing the perturbations of the steady motion in order to check the system stability, all perturbed motions should be considered as affected by different hysteretic coefficients $c_{hi} = h/\omega - d_h$, inversely proportional to the relative angular speed $|\omega - \omega|$ [10], but this approach would be scarcely productive for non-linear systems like the present one. Therefore, in the search of the stability limits, very small deviations from the main deformation of the shaft will be assumed and the changes of the viscous-equivalent coefficient $c_{hi} = h/\omega$ will be neglected in the calculation of the hysteretic force.

The amplitudes of the dry friction force vectors Φ_3 and Φ_4 are supposed constant and their components are given by $-\phi_j x'_j / \sqrt{x_j'^2 + y_j'^2}$ and $-\phi_j y'_j / \sqrt{x_j'^2 + y_j'^2}$ (for $j = 3, 4$). If one or both supports are sticking, the sliding force Φ_j must be replaced by the adhesive force $\Phi_{\text{adh.,}j}$ which must balance the other forces acting on the support. The dimensionless friction forces are scaled by ke : $\Phi_j = \phi_j/(ke)$ and $\Phi_{\text{adh.,}j} = \phi_{\text{adh.,}j}/(ke)$.

All displacements are scaled by the rotor eccentricity e , all rotations by e/l , all forces by ke and all moments by kel , whence, introducing the dimensionless displacement-rotation vectors $\mathbf{X} = \{X_1, X_2, X_3, X_4\}^T$ and $\mathbf{Y} = \{Y_1, Y_2, Y_3, Y_4\}^T$, where $X_j = x_j/e$, $Y_j = y_j/e$, for $j \neq 2$, $X_j = \psi/l/e$, $Y_j = -\phi/l/e$, for $j = 2$, the motion equations may be written in the form

$$\mathbf{KX} + 2\Omega\mathbf{DX}' + 2\mathbf{H}(\mathbf{X}' + \mathbf{Y}) + \Omega^2\mathbf{MX}'' + \Omega^2\mathbf{GY}' + \left\{ -\Omega^2 \cos \theta \quad 0 \quad \frac{\sigma_3 \Phi_3 X_3'}{\sqrt{X_3'^2 + Y_3'^2}} + (1 - \sigma_3) \Phi_{\text{adh.3,x}} \quad \frac{\sigma_4 \Phi_4 X_4'}{\sqrt{X_4'^2 + Y_4'^2}} + (1 - \sigma_4) \Phi_{\text{adh.4,x}} \right\}^T = 0 \quad (1x)$$

$$\mathbf{KY} + 2\Omega\mathbf{DY}' + 2\mathbf{H}(\mathbf{Y}' - \mathbf{X}) + \Omega^2\mathbf{MY}'' - \Omega^2\mathbf{GX}' + \Gamma \{1 \quad 0 \quad M_3 \quad M_4\}^T + \left\{ -\Omega^2 \sin \theta \quad 0 \quad \frac{\sigma_3 \Phi_3 Y_3'}{\sqrt{X_3'^2 + Y_3'^2}} + (1 - \sigma_3) \Phi_{\text{adh.3,y}} \quad \frac{\sigma_4 \Phi_4 Y_4'}{\sqrt{X_4'^2 + Y_4'^2}} + (1 - \sigma_4) \Phi_{\text{adh.4,y}} \right\}^T = 0 \quad (1y)$$

where the numbers σ_j denote the sliding ($\sigma_j = 1$) or adhesive ($\sigma_j = 0$) state of the dry friction contact, \mathbf{D} , \mathbf{M} and \mathbf{G} are the damping, massive and gyroscopic matrices, all diagonal, whose coefficients are (d_1, d_2, d_3, d_4) , $(1, J_d, M_3, M_4)$ and $(0, J_a, 0, 0)$ respectively, being J_d and J_a the dimensionless diametral and axial moment of inertia of the rotor, scaled by $m l^2$, while \mathbf{K} and \mathbf{H} are the symmetric stiffness and hysteretic matrices, which, for a hinged-hinged shaft, are given by

$$\mathbf{K} = \frac{1}{16L_3^3 L_4^3} \begin{bmatrix} 1 - 3L_3 L_4 & L_3 L_4 (L_3 - L_4) & -L_4^3 & -L_3^3 \\ L_3 L_4 (L_3 - L_4) & L_3^2 L_4^2 & L_3 L_4^3 & -L_4 L_3^3 \\ -L_4^3 & L_3 L_4^3 & 16L_3^3 L_4^3 K_3 + L_4^3 & 0 \\ -L_3^3 & -L_4 L_3^3 & 0 & 16L_3^3 L_4^3 K_4 + L_3^3 \end{bmatrix} \quad (2)$$

$$\mathbf{H} = d_h \begin{bmatrix} 1 & 0 & -L_4 & -L_3 \\ 0 & 0 & 0 & 0 \\ -L_4 & 0 & L_4^2 & L_3 L_4 \\ -L_3 & 0 & L_3 L_4 & L_3^2 \end{bmatrix} \quad (3)$$

The constant part of the solution, i. e. the equilibrium configuration of the rotor, can be easily obtained by Eqs. (1) and this solution is clearly not unique in case of adhesive contact between the friction surfaces. For sliding contacts or else for continuous sliding-adhesion transition, one gets $\mathbf{X}_{\text{equil.}} = 2\Gamma\mathbf{AH}(\mathbf{K} + 4\mathbf{HAH})^{-1}\{1, 0, M_3, M_4\}^T$, $\mathbf{Y}_{\text{equil.}} = -\Gamma(\mathbf{K} + 4\mathbf{HAH})^{-1}\{1, 0, M_3, M_4\}^T$, where $\mathbf{A} = \mathbf{K}^{-1}$ is the flexibility matrix and, as $\mathbf{X}_{\text{equil.}} \neq 0$, a static bias due to hysteresis is observable. Yet, in the following, the vectors \mathbf{X} and \mathbf{Y} will be assumed emptied of their constant content, $\mathbf{X}_{\text{equil.}}$, $\mathbf{Y}_{\text{equil.}}$.

The dynamic part of Eqs. (1) can be compacted multiplying Eqs. (1y) by the unit imaginary number i , summing them to Eqs. (1x) and putting $\mathbf{W} = \mathbf{X} + i\mathbf{Y}$, $\hat{\Phi}_{\text{adh.}j} = \Phi_{\text{adh.}j,x} + i\Phi_{\text{adh.}j,y}$:

$$\mathbf{KW} + 2\Omega\mathbf{DW}' + 2\mathbf{H}(\mathbf{W}' - i\mathbf{W}) + \Omega^2\mathbf{MW}'' - i\Omega^2\mathbf{GW}' + \left\{ -\Omega^2 \exp(i\theta) \quad 0 \quad \sigma_3 \Phi_3 \exp(i \arg W_3') + (1 - \sigma_3) \hat{\Phi}_{\text{adh.3}} \quad \sigma_4 \Phi_4 \exp(i \arg W_4') + (1 - \sigma_4) \hat{\Phi}_{\text{adh.4}} \right\}^T = 0 \quad (4)$$

The natural whirling modes are circular and can be derived cancelling the matrices \mathbf{D} , \mathbf{H} and the gravitational-unbalance force vector. Using the complex notation $\mathbf{W} = \mathbf{W}_0 \exp(i\Omega_n \theta / \Omega)$, where $\Omega_n = \omega_n / \omega_c$ is the dimensionless precession speed, we get $[\mathbf{K} - \Omega_n^2(\mathbf{M} - \mathbf{G}\Omega / \Omega_n)]\mathbf{W}_0 = \mathbf{Z}(\Omega, \Omega_n)\mathbf{W}_0 = 0$, where $\mathbf{Z}(\Omega, \Omega_n)$ is a dynamical matrix for the natural motions. Extracting the

characteristic polynomial, an eight degree algebraic equation is obtained for Ω_n , whose coefficients are functions of Ω . Putting $I = J_d - J_a \Omega / \Omega_n$ for brevity and indicating the cofactors with the superscripts ...^(c), one gets $(K_{22} - I \Omega_n^2) Z_{22}^{(c)} + K_{12} Z_{12}^{(c)} + K_{32} Z_{32}^{(c)} + K_{42} Z_{42}^{(c)} = 0$. The characteristic roots, that is the natural precession speeds, may be traced on conventional Campbell diagrams $\Omega_n(\Omega)$. Figure 2 shows two example cases, for an oblong and an oblate ellipsoid of inertia of the rotor, and eight branches of the locus are visible on each diagram, characterised by an asymptote with slope J_a / J_d and seven other horizontal asymptotes, given by $\Omega_n = 0$ and by the roots of the equation $Z_{22}^{(c)} = 0$, which is cubic in Ω_n^2 . The critical angular speeds, $\Omega_n = \pm \Omega$, are identified by the intersection of the locus with the bisectors of the axes, where the minus sign refers to the critical retrograde precession (see Stodola and Den Hartog). There are eight or seven critical speeds for $J_a / J_d < 1$ or $J_a / J_d > 1$ respectively (oblong or oblate ellipsoid of inertia of the rotor).

3. STEADY WHIRLING MOTIONS

The steady circularly polarized solution can be obtained putting $\mathbf{W} = \mathbf{W}_0 \exp(i\theta)$ into Eqs. (4), observing that the hysteretic terms vanish, and rewriting Eq. (4) in the form

$$\begin{aligned} & \left[\mathbf{K} + 2i\Omega \mathbf{D} - \Omega^2 (\mathbf{M} - \mathbf{G}) \right] \mathbf{W}_0 = (\mathbf{Z}_0 + 2i\Omega \mathbf{D}) \mathbf{W}_0 = \mathbf{Z} \mathbf{W}_0 = \\ & = \left\{ \Omega^2 \quad 0 \quad -i\sigma_3 \Phi_3 \exp(i \arg W_{0,3}) - (1 - \sigma_3) \bar{\Phi}_{\text{adh},3} \quad -i\sigma_4 \Phi_4 \exp(i \arg W_{0,4}) + (1 - \sigma_4) \bar{\Phi}_{\text{adh},4} \right\}^T \end{aligned} \quad (5)$$

where \mathbf{Z} is a complex impedance matrix, \mathbf{Z}_0 its real non-viscous part and $\bar{\Phi}_{\text{adh},j}$ gives the complex amplitudes of the dimensionless adhesion force.

Since the coefficients of matrix \mathbf{Z} are real and symmetric in all the off-diagonal places, due to the diagonal nature of matrix \mathbf{D} , indicating with i, j, k, l a generic combination of the subscripts 1, 2, 3, 4, without repetition, the cofactors and determinant of \mathbf{Z} can be found to be expressed by $Z^{(c)}_{ii}$

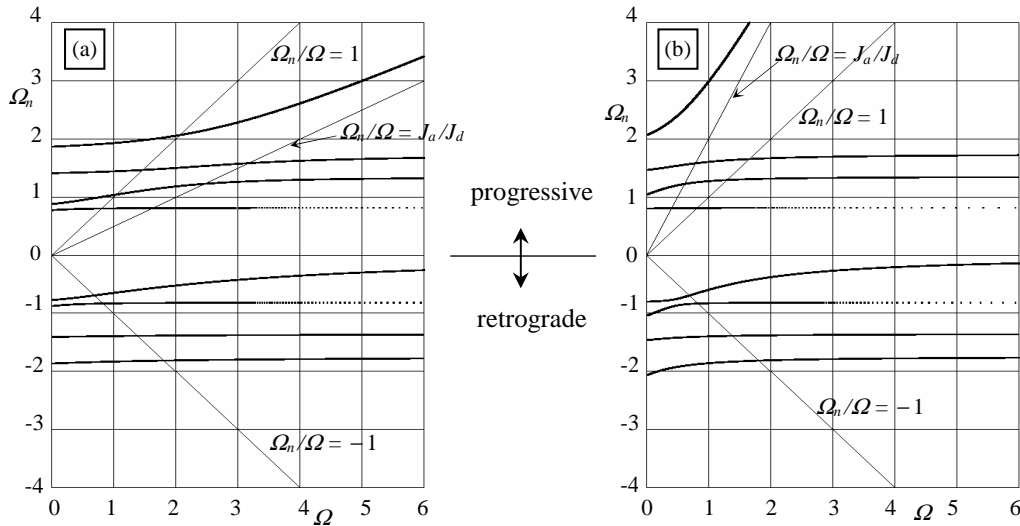


Figure 2: Campbell diagrams $\Omega_n(\Omega)$ for $L_3 = 0.4$, $K_3 = K_4 = 1.5$, $M_3 = M_4 = 1$
(a): $J_a = 0.1$, $J_d = 0.2$ (oblong inertia ellipsoid) - (b): $J_a = 0.2$, $J_d = 0.1$ (oblate inertia ellipsoid)

$$\begin{aligned}
= & Z_{0,ii}^{(c)} - 4 \Omega^2 \sum_{j \neq k \neq l} d_j d_k Z_{0,ll} + 2 i \Omega \left[\sum_{j \neq k \neq l} d_j (Z_{0,kk} Z_{0,ll} - Z_{0,lk}^2) - 4 \Omega^2 d_j d_k d_l \right], \quad Z_{ij}^{(c)} = Z_{0,ij}^{(c)} \\
& - 4 \Omega^2 d_k d_l Z_{0,ij} - 2 i \Omega \left[d_k (Z_{0,ij} Z_{0,ll} - Z_{0,il} Z_{0,jl}) + d_l (Z_{0,ij} Z_{0,kk} - Z_{0,ik} Z_{0,jk}) \right], \det(\mathbf{Z}) = \det(\mathbf{Z}_0) + \\
& - 4 \Omega^2 \sum_{i \neq j \neq k \neq l} d_i d_j (Z_{0,kk} Z_{0,ll} - Z_{0,kl}^2) + 16 \Omega^4 d_1 d_2 d_3 d_4 + 2 i \Omega \left[\sum_i d_i Z_{0,ii}^{(c)} - 4 \Omega^2 \sum_{i \neq j \neq k \neq l} d_i d_j d_k Z_{0,ll} \right] \text{ and the}
\end{aligned}$$

complex matrix inversion, $\mathbf{Z}^{-1} = [\mathbf{Z}_{ij}^{(c)}]^T / \det(\mathbf{Z})$, permits calculating the complex vector $\mathbf{W}_0 = \mathbf{Z}^{-1} \left\{ \Omega^2 \quad 0 \quad -i \sigma_3 \Phi_3 \exp(i \arg W_{0,3}) - (1 - \sigma_3) \bar{\Phi}_{\text{adh},3} \quad -i \sigma_4 \Phi_4 \exp(i \arg W_{0,4}) + (1 - \sigma_4) \bar{\Phi}_{\text{adh},4} \right\}^T$, where it is convenient to put $W_{0,j} = R_j \exp(-i \gamma_j)$, R_j being the real orbital radii. If there is adhesion between the friction surfaces of any support ($\sigma_j = 0$), the sliding term $-i \Phi_j \exp(-i \gamma_j)$, whose only argument is unknown, must be replaced by the adhesive term $-\bar{\Phi}_{\text{adh},j}$, with unknown argument and modulus, but the addition of an extra unknown is compensated by the vanishing of the radius R_j . Therefore, it is convenient to replace the exponential term $\exp(-i \gamma_j)$ with a more general complex friction number \hat{N}_j , whose modulus and argument are 1 and $-\gamma_j$ for $R_j > 0$, but are both unknown for $R_j = 0$, where $|\hat{N}_j|$ is equal to the adhesive-to-sliding force ratio.

The solution can be written down in the form

$$\begin{aligned}
R_1 \exp(-i \gamma_1) = c_{10} - i c_{13} \hat{N}_3 - i c_{14} \hat{N}_4 & \quad R_2 \exp(-i \gamma_2) = c_{20} - i c_{23} \hat{N}_3 - i c_{24} \hat{N}_4 \\
R_3 \exp(-i \gamma_3) = c_{30} - i c_{33} \hat{N}_3 - i c_{34} \hat{N}_4 & \quad R_4 \exp(-i \gamma_4) = c_{40} - i c_{43} \hat{N}_3 - i c_{44} \hat{N}_4
\end{aligned} \tag{6_{1,2,3,4}}$$

where the coefficients $c_{ij} = c_{ij,r} + i c_{ij,i}$ are complex in general, but become real in the absence of viscous dissipation ($c_{ij,i} = 0$).

Fixing the rotor angular speed, the solution procedure is similar to [6], as summarised hereafter. Assuming firstly sliding conditions for both the journal boxes, one puts $\hat{N}_j = \exp(-i \gamma_j)$ and solves Eqs. (6) for the eight quantities R_j and γ_j . If no couple of real positive solutions for R_3 and R_4 can be found, one or both the journal boxes are stuck and new solutions are sought in the hypothesis of adhesion of the one or the other support, putting either $R_3 = 0$ or $R_4 = 0$ and calculating the complex number \hat{N}_3 or \hat{N}_4 and the orbital radius R_4 or R_3 of the other sliding support. If positive radii cannot yet be found, there are stick conditions on both supports and the numbers \hat{N}_j are calculated putting $R_3 = R_4 = 0$. In the case of two possible whirling motions, the one with adhesion of support 3 and the other of support 4, the solution giving a continuous transition from the sliding to the stick state or vice versa has to be chosen.

Using the above procedure, an optimization process may be carried out in order to minimize the whirling motion in the best manner. In practice, fixing some specific optimization weights for the motion amplitudes of the rotor and the supports, the maximum value of their weighted average is minimized throughout the speed range. This optimization process may be carried out numerically, varying the two variables Φ_3 and Φ_4 gradually, spanning the critical speed range at each step and reducing the step size in the close neighbourhood of the minimum of the above maximum weighted average.

Figures 3_{1,2,3,4} show the optimized speed response of the rotor (R_1, R_2) and the supports (R_3, R_4) for an example case with no external damping. The rotor response in the two cases of fixed-fixed and floating-floating journal boxes are also shown and it is possible to appreciate the good

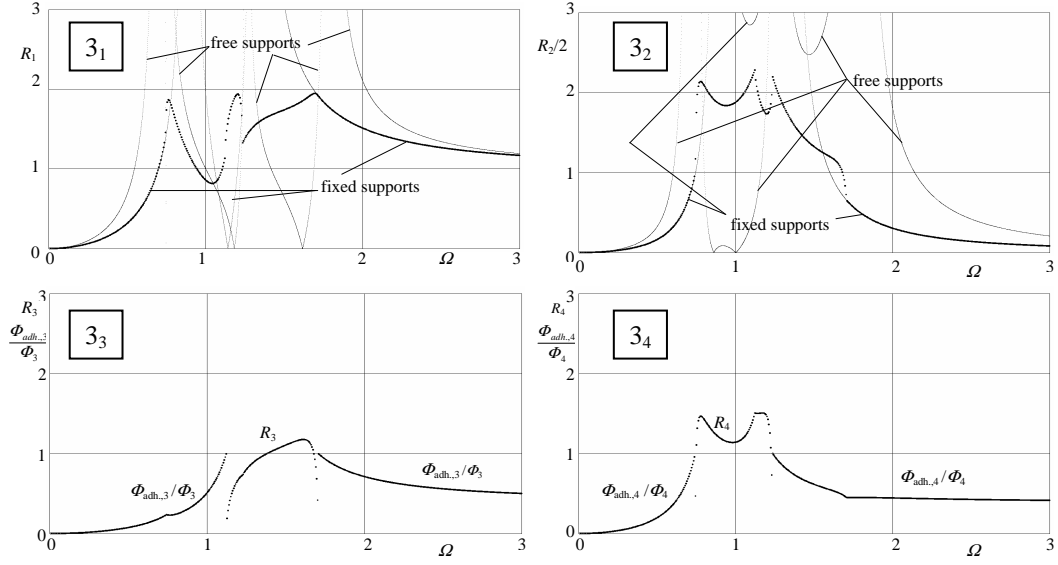


Figure 3_{1,2,3,4}: Optimised frequency response for hinged-hinged rotor-shaft system.

Data: $\Phi_3 = 2.4054688$, $\Phi_4 = 0.746875$, $w_1 = w_2 = 0.3$, $w_3 = w_4 = 0.2$

Data: $L_3 = 0.4$, $d_1 = d_2 = d_3 = d_4 = 0$, $K_3 = K_4 = 1$, $M_3 = M_4 = 1$, $J_d = 0.4$, $J_a = 0.2$

efficiency of the dry friction dampers in cutting all critical speeds by getting into an adhesive state and in restraining the whirl amplitude in the remaining range. Figures 3_{3,4} show also the adhesive force level in the stuck range.

4. STABILITY

The stability of the steady motion “in the small” can be inspected by the small perturbation approach. Assuming that a perturbation, $\tilde{\mathbf{X}}$, $\tilde{\mathbf{Y}}$, is superimposed to the steady solution (without the tilde), one gets by Eq. (1), in the hypothesis of full sliding of both supports,

$$\mathbf{K}\tilde{\mathbf{X}} + 2\Omega\mathbf{D}\tilde{\mathbf{X}}' + 2\mathbf{H}(\tilde{\mathbf{X}}' + \tilde{\mathbf{Y}}) + \Omega^2(\mathbf{M}\tilde{\mathbf{X}}'' + \mathbf{G}\tilde{\mathbf{Y}}') = \left\{ \begin{array}{c} 0 \\ 0 \\ \Phi_3 \left[\frac{X_3'}{\sqrt{X_3'^2 + Y_3'^2}} - \frac{X_3' + \tilde{X}_3'}{\sqrt{(X_3' + \tilde{X}_3')^2 + (Y_3' + \tilde{Y}_3')^2}} \right] \\ \Phi_4 \left[\frac{X_4'}{\sqrt{X_4'^2 + Y_4'^2}} - \frac{X_4' + \tilde{X}_4'}{\sqrt{(X_4' + \tilde{X}_4')^2 + (Y_4' + \tilde{Y}_4')^2}} \right] \end{array} \right\}^T \quad (7x)$$

$$\mathbf{K}\tilde{\mathbf{Y}} + 2\Omega\mathbf{D}\tilde{\mathbf{Y}}' + 2\mathbf{H}(\tilde{\mathbf{Y}}' - \tilde{\mathbf{X}}) + \Omega^2(\mathbf{M}\tilde{\mathbf{Y}}'' - \mathbf{G}\tilde{\mathbf{X}}') = \left\{ \begin{array}{c} 0 \\ 0 \\ \Phi_3 \left[\frac{Y_3'}{\sqrt{X_3'^2 + Y_3'^2}} - \frac{Y_3' + \tilde{Y}_3'}{\sqrt{(X_3' + \tilde{X}_3')^2 + (Y_3' + \tilde{Y}_3')^2}} \right] \\ \Phi_4 \left[\frac{Y_4'}{\sqrt{X_4'^2 + Y_4'^2}} - \frac{Y_4' + \tilde{Y}_4'}{\sqrt{(X_4' + \tilde{X}_4')^2 + (Y_4' + \tilde{Y}_4')^2}} \right] \end{array} \right\}^T \quad (7y)$$

If one support is stuck, the correspondent static friction force is unknown, but the amplitude of its motion is zero, so that the number of degrees of freedom is reduced. If both journal boxes are stuck, the system becomes linear with constant coefficients, so that the stability may be controlled

by the conventional Routh-Hurwitz procedure.

Assuming only small perturbations, the linear approximation of the friction terms of Eqs. (7) yields $\Phi_j \frac{Y_j(Y_j\tilde{X}'_j - X'_j\tilde{Y}'_j)}{(X_j'^2 + Y_j'^2)\sqrt{X_j'^2 + Y_j'^2}}$ into (7x), $\Phi_j \frac{X'_j(X'_j\tilde{Y}'_j - Y'_j\tilde{X}'_j)}{(X_j'^2 + Y_j'^2)\sqrt{X_j'^2 + Y_j'^2}}$ into (7y) and recalling the results of the previous section, the 4 + 4 equations of the differential system (7x,y) can be transformed into the 8 + 8 first order differential equations with variable coefficients

$$\begin{aligned}
\tilde{\mathbf{X}}' &= \tilde{\mathbf{U}} \\
\tilde{\mathbf{Y}}' &= \tilde{\mathbf{V}} \\
\tilde{\mathbf{U}}' &= -\frac{\mathbf{M}^{-1}}{\Omega^2} \left[\mathbf{K}\tilde{\mathbf{X}} + 2\mathbf{D}\tilde{\mathbf{U}} + 2\mathbf{H}(\tilde{\mathbf{U}} + \tilde{\mathbf{Y}}) + \Omega^2\mathbf{G}\tilde{\mathbf{V}} + \right. \\
&+ \left. \begin{Bmatrix} 0 & 0 & \frac{\Phi_3}{R_3} [\tilde{U}_3 \cos^2(\theta - \gamma_3) + \tilde{V}_3 \sin(\theta - \gamma_3) \cos(\theta - \gamma_3)] & \frac{\Phi_4}{R_4} [\tilde{U}_4 \cos^2(\theta - \gamma_4) + \tilde{V}_4 \sin(\theta - \gamma_4) \cos(\theta - \gamma_4)] \end{Bmatrix}^T \right] \quad (8) \\
\tilde{\mathbf{V}}' &= -\frac{\mathbf{M}^{-1}}{\Omega^2} \left[\mathbf{K}\tilde{\mathbf{Y}} + 2\mathbf{D}\tilde{\mathbf{V}} + 2\mathbf{H}(\tilde{\mathbf{U}} - \tilde{\mathbf{X}}) - \Omega^2\mathbf{G}\tilde{\mathbf{U}} + \right. \\
&+ \left. \begin{Bmatrix} 0 & 0 & \frac{\Phi_3}{R_3} [\tilde{V}_3 \sin^2(\theta - \gamma_3) + \tilde{U}_3 \sin(\theta - \gamma_3) \cos(\theta - \gamma_3)] & \frac{\Phi_4}{R_4} [\tilde{V}_4 \sin^2(\theta - \gamma_4) + \tilde{U}_4 \sin(\theta - \gamma_4) \cos(\theta - \gamma_4)] \end{Bmatrix}^T \right]
\end{aligned}$$

Introducing the 16-dimensional state vector $\tilde{\mathbf{S}} = \{\tilde{\mathbf{X}}, \tilde{\mathbf{Y}}, \tilde{\mathbf{U}}, \tilde{\mathbf{V}}\}^T$ and indicating the 16×16 system matrix of Eqs. (8) by \mathbf{T} , Equations (8) appear in the form $\tilde{\mathbf{S}}' = \mathbf{T}(\theta)\tilde{\mathbf{S}}$.

Due to the non-constancy of matrix \mathbf{T} , whose coefficients are periodic in θ with period π , the Floquet theory may be applied to ascertain the stable or unstable nature of the slightly perturbed motion [11]. It is necessary to derive firstly the 16×16 fundamental matrix solution $\Theta(\theta)$, equal to the identity matrix \mathbf{I} for $\theta = 0$, which can be done by means of some routine of the Euler-Cauchy type or of the Runge-Kutta type. Then, the eigenvalues of $\Theta(\theta)$ after one period (also called characteristic multipliers) must be extracted by the 16th degree characteristic equation $E_c(\lambda) = \det[\Theta(\pi) - \lambda\mathbf{I}] = \lambda^{16} + b_1\lambda^{15} + \dots + b_{15}\lambda + b_{16} = 0$. Stability requires all these characteristic multipliers to be smaller than one in modulus.

If one support, say j , is stuck to the frame, all the terms of the correspondent rows ($X'_j \rightarrow, Y'_j \rightarrow, U'_j \rightarrow, V'_j \rightarrow$) and columns ($X_j \downarrow, Y_j \downarrow, U_j \downarrow, V_j \downarrow$) of $\Theta(\pi)$ are replaced by zeroes, so that a factor λ^4 arises naturally in the characteristic equation, $E_c(\lambda) = \lambda^4(\lambda^{12} + b_1\lambda^{11} + \dots)$, which is uninfluential on the system stability as point $\lambda = 0$ is just the centre at the unitary circle in the Gauss-Argand plane. If both supports are stuck, the differential system reduces to the constant coefficient form and it is sufficient to check the stability by the Routh-Hurwitz criterion. All these occurrences can be automatically controlled by some suitable computational procedure.

The coefficients b_j of the characteristic polynomial E_c can be obtained by a collocation type procedure, once calculating the matrix $\Theta_\pi = \Theta(\pi)$. Since $b_1 = -\text{Tr}(\Theta_\pi)$ and $b_{16} = \det(\Theta_\pi)$ can be quickly calculated, the other fourteen coefficients are obtainable choosing seven distinct numbers n , e. g. $n = 1, 2, 3, 4, 5, 6, 7$, and writing $b_2n^{14} + b_3n^{13} + \dots + b_{14}n^2 + b_{15}n = -\det(\Theta_\pi) + \text{Tr}(\Theta_\pi)n^{15} - n^{16} + E_c(n)$, $b_2n^{14} - b_3n^{13} + \dots + b_{14}n^2 - b_{15}n = -\det(\Theta_\pi) - \text{Tr}(\Theta_\pi)n^{15} - n^{16} + E_c(-n)$, where the quantities $E_c(n)$ and $E_c(-n)$ are easily calculable by numerics.

Summing and subtracting such equations for each n , one gets two algebraic systems, for the even and odd coefficients respectively, $b_2n^{14} + b_4n^{12} + \dots + b_{14}n^2 = -\det(\Theta_\pi) - n^{16} +$

$$[E_c(n) + E_c(-n)]/2, b_3 n^{13} + b_5 n^{11} + \dots + b_{15} n = \text{Tr}(\Theta_\pi) n^{15} + [E_c(n) - E_c(-n)]/2.$$

Actually, once obtaining the development of the polynomial $E_c(\lambda)$, there is no need to calculate its roots, but it is sufficient, for the stability analysis, to verify that they lie inside the unit circle of the complex plane. Since $E_c(\lambda) = (\lambda - \lambda_1)(\lambda - \lambda_2)(\lambda - \lambda_3) \dots (\lambda - \lambda_{16})$ is equal to the product of sixteen complex vectors $(\lambda - \lambda_j)$, when the variable λ moves counter-clockwise along the unit circle, starting from the real axis and reaching the starting position at the end of one complete turn, the argument of its conformal image $E_c[\exp(i\phi)]$ increases of sixteen times 2π if all the roots λ_j remain on the left of this trajectory, otherwise it performs a lesser number of turns, if some roots lie outside the unit circle. Fixing the system parameters, the numerical check of stability requires just a short time on a common PC and the process may be re-iterated changing some mechanical characteristic, for example until the stability threshold is attained.

Figure 4 shows the total viscous damping level needed to assure a stable rotating motion, together with the changes of the speed response, for the optimized rotor-shaft system described by Fig. 3. As observable, just a small amount of damping is requested to stabilize the shaft rotation above the first critical speed, and this amount is largely reduced in the sliding range of the response curves can be observed, so that the analysis leading to Fig. 3, which neglects the viscous damping, is acceptable with a sufficient approximation.

At this point, an important consideration has to be made. As the above approach refers to small perturbations of the main motion, nothing can be concluded about the stability “in the large”. Moreover, in case of sticking support, the instability of the steady motion leads necessarily to release the adhesive contact between the friction surfaces and the arising sliding forces have a strong stabilising influence. Unfortunately, the stability “in the large” can be inspected only by the direct numerical solution of the differential system, e. g. by some Runge-Kutta routine, starting for example from random initial conditions and proceeding as far as a large number of cycles are completed (100 or more). The result is that the unstable whirling motion does not lead at all to divergent conditions, as could be predicted by the linear analysis, but simply to a sort of small wobbling of the trajectories of the rotor and the support in the neighbourhood of their steady circular attractor. This asymptotic behaviour is clearly visible in Fig. 5, which refers to a solution for particular conditions that are otherwise unstable “in the small”.

Summing up, the dry friction dampers exert a very important restraining effect on all the small unstable whirling motions that may arise throughout the entire speed range, in the sense that the unstable trembling motion is limited to a wandering of the trajectory amplitude in the very close neighbourhood of the steady circular path. Nevertheless, if the operative conditions of the rotor-shaft-suspension system are planned for the adhesive supercritical regime, such trembling motion of the supports is not convenient, due to the increase of wear and heat production, and thus, it is

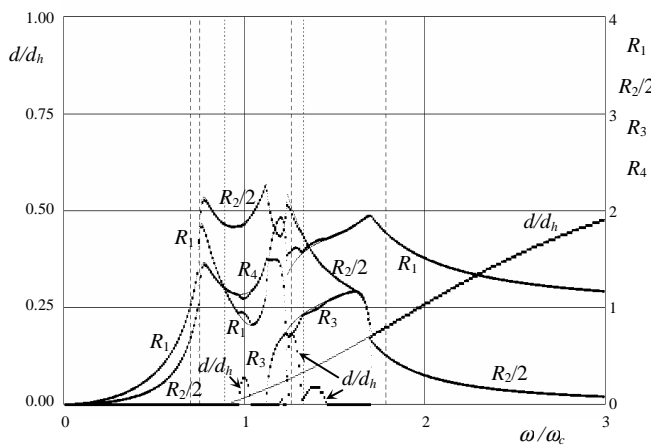


Figure 4: Viscous damping at stability threshold.
 $d_h = 0.05, d_1 = d_2 = d_3 = d_4 = d$; other data like in Fig. 3

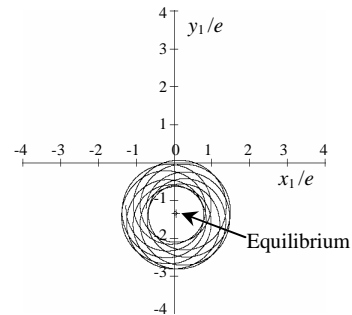


Figure 5: Non-periodic rotor centre path.
 $K_3 = K_4 = M_3 = M_4 = 0.2, J_d = 0.4, J_a = 0.2$
 $d_h = 0.1, d_1 = d_2 = d_3 = d_4 = 0.25 \times d_h$
 $\omega/\omega_c = 4, L_3 = 0.4, \Gamma = 0.3$
 $\Phi_3 = 1.3160156, \Phi_4 = 0.39335938$
 (interval: 20 cycles)

better that the journal boxes remain stuck to the frame and the stability is achieved by the other external dissipative sources.

Moreover, it is remarkable that the hysteretic stabilization may be also obtained by anisotropic stiffness characteristics of the supports in the horizontal and vertical planes (see [12]).

6. CONCLUSION

The problem of the hysteretic instability of the whirling motion in rotating machinery has to be faced by different approaches depending on the linear or non-linear nature of the system characteristics. For example, in the hypothesis of floating journal boxes with dry friction surfaces, planned to damp the critical speeds, the stability of the periodic solutions requires applying the Floquet theory, which implies the numerical calculation of the fundamental solution matrix and the control that the characteristic multipliers are confined into the unitary circle of the Gauss-Argand plane. In the range of the adhesive contact on the contrary, it is convenient to apply the Routh-Hurwitz criterion. On the other hand, the stability “in the large” can be controlled only by the numerical solution of the full equations.

References

- [1] Kirk, R.G. and Gunter, E.J., “The Effect of Support Flexibility and Damping on the Synchronous Response of a Single-Mass Flexible Rotor”, *ASME J. Engineering for Industry*, **94**, 221-232 (1972).
- [2] Kirk, R.G. and Gunter, E.J., “Effect of Support Flexibility and Damping on the Dynamic Response of a Single-Mass Flexible Rotor in Elastic Bearings”, *NASA CR-2083*, July 1972.
- [3] Guo, Z. and Kirk, R.G., “Theoretical Study on Instability Boundary of Rotor-Hydrodynamic Bearing Systems: Part I—Jeffcott Rotor with External Damping”, *ASME J. of Vibration and Acoustics*, **125**, 417-422 (2003).
- [4] Guo, Z. and Kirk, R.G., “Theoretical Study on Instability Boundary of Rotor-Hydrodynamic Bearing Systems: Part II—Rotor with External Flexible Damped Support”, *ASME J. of Vibration and Acoustics*, **125**, 423-426 (2003).
- [5] Sorge, F., “Rotor Whirl Damping by Dry Friction Suspension Systems”, *MECCANICA*, Springer, **43**, n. 6, pp. 577-589 (2008).
- [6] Sorge, F., “Damping of Rotor Conical Whirl by Asymmetric Dry Friction Suspension”, *Journal of Sound and Vibr.*, **321** (1-2), pp. 79-103 (20/03/2009)
- [7] Kirk, R.G. and Hornschuch, H., “*Bearing and Housing Assembly*”, U.S. Patent n. 4119375, Oct. 10, 1978.
- [8] Moringiello, D.C. and Dallmann, S.H., “*Friction Damper*”, U.S. Patent n. 4337982, Jul. 6, 1982.
- [9] Montagnier, O. and Hochard, Ch., “Dynamic Instability of Supercritical Driveshafts Mounted on Dissipative Supports—Effects of Viscous and Hysteretic Internal Damping”, *J. of Sound and Vibr.*, **305**, 378–400 (2007).
- [10] Wettergren, H.L., “On the Behavior of Material Damping Due to Multi-Frequency Excitation”, *J. of Sound and Vibr.*, **206**, 725-735 (1997).
- [11] Nayfeh, A.H. and Mook, D.T., “*Nonlinear Oscillations*”, John Wiley & Sons, New York, U.S.A., 1979.
- [12] Sorge, F. and Cammalleri, M., “An Efficient Damping Technique for the Unstable Hysteretic Rotor Whirl by Proper Suspension Systems”, *ECOTRIB 2009, European Conference on Tribology*, Pisa, Italy, June 7-10, 2009.